Sensitivity of Actively Damped Structures to Imperfections and Modeling Errors

Raphael T. Haftka* and Rakesh K. Kapania†
Virginia Polytechnic Institute and State University, Blacksburg, Virginia

The sensitivity of actively damped response of structures with respect to errors in the structural modeling is studied. Two ways of representing errors are considered. The first approach assumes errors in the form of spatial variations (or imperfections) in the assumed mass and stiffness properties of the structures. The second approach assumes errors due to such factors as unknown joint stiffnesses, discretization errors, and nonlinearities. These errors are represented here as discrepancies between experimental and analytical mode shapes and frequencies. The actively damped system considered here is a direct-rate feedback regulator based on a number of colocated velocity sensors and force actuators. The response of the controlled structure is characterized by the eigenvalues of the closed-loop system. The effects of the modeling errors are thus presented as the sensitivity of the eigenvalues of the closed-loop system. Results are presented for two examples: 1) a three-span simply supported beam controlled by three sensors and actuators, and 2) a laboratory structure consisting of a cruciform beam supported by cables.

Introduction

A GREAT deal of research is currently in progress on the design of active control systems for large space structures.[1] This is due to the fact that because of the requirement for low weight, large space structures will lack the stiffness and damping required for adequate passive control of vibrations. Control systems are generally designed by assuming that the geometry and stiffness of the structure is known and its response is linear. The actual structures may have some nonlinearities (e.g., at the joints), and also have slightly different geometric and stiffness parameters from those assumed during the design of the controllers.

For some large space structures, the errors in modeling the stiffness and inertial characteristics may significantly affect the controller design. For all such cases, it is of interest to study the sensitivity of the response of the controlled structure to the errors in the structural model.

Previously, a number of studies have been conducted to study the effect of small structural modifications on the controllability[2,3] and on the free vibrations response[4] of the structures. Haftka et al.[2] presented a procedure to find out if small changes in a structure have the potential for significant enhancements of its vibration control system. The procedure consisted of two steps. In the first step, the sensitivity of the required strength of the control system to small changes in the structural parameters was obtained. In the second step, an optimization procedure was used to produce maximum reduction in the required control system strength with minimum change in the structural configuration.

In a subsequent study, Haftka et al.[3] extended the work of Ref. 2 by assuming that the control system is optimized for maximum performance for the original structural configuration and then reoptimized to take full advantage of the structural modifications. Sensitivity analysis of the optimized systems was used to predict the changes in the control system required to take full advantage of the structural modifications and the ensuing change in performance.

The present paper is concerned with the sensitivity of the controlled response of the structure with respect to errors in the structural model.

Two ways of representing errors are considered. The first approach assumes errors in the form of spatial variations (or imperfections) in the assumed mass and stiffness properties of the structures. This approach is applicable to assessing the effect of inaccuracies in the manufacturing process based on estimates of the magnitude of such inaccuracies. The second approach is directed towards modeling errors due to more complex factors such as unknown joint stiffnesses, discretization errors, and nonlinearities. These errors are typically detected by discrepancies between experimental and analytical mode shapes and natural frequencies. Therefore, these errors are represented here by variations in the mode shapes and frequencies of the uncontrolled structure.

The present work is limited to a simple linear direct-rate feedback regulator based on a number of colocated velocity sensors and force actuators. In that case the control action can be represented by a damping matrix. The response of the structure is discretized by modal expansion. The response of the controlled structure is characterized by the eigenvalues of the closed-loop system, so that the effects of modeling errors are presented as the sensitivity of these eigenvalues.

Two examples are considered. In the first example, a three-span simply supported beam controlled by three sensors and three actuators is used. The sensitivity of the controlled beam to spatial variations of the width and thickness of the beam is studied. The second example consists of a flexible beam supported by four cables and is controlled by a rate feedback, three-colocated force-actuator velocity-sensor pairs.

Sensitivity of Damped Structural Response

Errors in Terms of Modal Parameters

It is assumed here that estimates of the model errors in terms of the frequencies and mode shapes of the natural vibration modes are known. It is desired to calculate the effect of these errors on the damped response characteristics. If the modal

Received Aug. 29, 1988; revision received Feb. 3, 1989.

*Christopher Kraft Professor, Department of Aerospace and Ocean Engineering. Member AIAA.

†Assistant Professor, Department of Aerospace and Ocean Engineering. Member AIAA.

errors are known accurately (e.g., from good experimental measurement), then the equations derived below would allow correction to the calculated damped characteristics. If, on the other hand, the information on modal errors is incomplete and not very accurate, then the results below can be used to estimate the magnitude of the expected error in the damped characteristics. The error in the ith natural frequency is denoted by e_i; that is, the frequency ω_i is given as

$$\omega_i = \omega_{mi} + e_i \tag{1}$$

where ω_{mi} is the frequency calculated from the structural model. Similarly, the vibration modes of the structure are expressed in terms of the vibration modes of the model as

$$\phi_i = \phi_{mi} + \sum_j e_{ij}\phi_{mj} \tag{2}$$

where ϕ_i and ϕ_{mi} are the vibration modes of the actual structure and the model, respectively.

In order to evaluate the effect of these modal errors on the damped response, we assume that the behavior of the structure can be obtained accurately from a discretized model. Furthermore, we limit ourselves to the case of direct-rate feedback colocated sensors and actuators where the effect of the control system can be represented by a damping matrix.

In terms of an error-free model, the equation of motion of the structure is

$$M\ddot{U} + C\dot{U} + KU = 0 \tag{3}$$

where U is the displacement vector and M, C, and K are the mass, damping, and stiffness matrix, respectively. The damped vibration modes are of the form

$$U = ue^{\lambda t} \tag{4}$$

so that the eigenvalues λ_r and corresponding eigenvectors u_r of the system are obtained by solving the quadratic eigenvalue problem

$$\lambda^2 Mu + \lambda Cu + Ku = 0 \tag{5}$$

We are interested in the effect of modeling errors in the mass, damping, and stiffness matrices on the eigenvalues of Eq. (5), and we denote these errors as M_E, C_E, and K_E, respectively. When λ_r is a distinct eigenvalue, and the errors are small, it is easy to check that the error λ_{rE} in the rth eigenvalue can be approximated as

$$\lambda_{rE} = -\frac{\lambda_r^2 u_r^T M_E u_r + \lambda_r u_r^T C_E u_r + u_r^T K_E u_r}{2\lambda_r u_r^T M u_r + u_r^T C u_r} \tag{6}$$

Since it is impossible to infer damping-matrix errors from known errors in undamped frequencies and mode shapes, we set $C_E = 0$. To be able to use Eq. (6), we need to express M_E and K_E in terms of the modal errors. The discretized form of Eq. (2) is

$$\phi = \phi^m + \phi^m E^T = \phi^m(I + E^T) \tag{7}$$

where ϕ and ϕ^m are matrices with columns consisting of the vibration modes of the real structure and the available model, respectively. We assume that the vibration modes of the structure are normalized with respect to the mass matrix, so that

$$\phi^T M \phi = I \tag{8}$$

so that from Eqs. (7) and (8),

$$M^{-1} = \phi\phi^T = \phi^m(I + E^T)(I + E)\phi^{mT} \tag{9}$$

Assuming that ϕ^m is also normalized with respect to the model mass matrix M_m and neglecting second-order error terms, we get

$$(M^{-1})_E = \phi^m \bar{E} \phi^{mT} \tag{10}$$

where $(M^{-1})_E$ is the error in M^{-1}, and $\bar{E} = E + E^T$. The error in the mass matrix M_E is related to the error in the inverse as

$$I = MM^{-1} = (M^m + M_E)[M^{m^{-1}} + (M^{-1})_E] \tag{11}$$

so that, neglecting second-order error terms,

$$M_E = -M^m(M^{-1})_E M^m = -M^m \phi^m \bar{E} \phi^{mT} M^m \tag{12}$$

The error in the stiffness matrix is obtained by using the relation

$$\phi^T K \phi = \Omega \tag{13}$$

where Ω is a diagonal matrix with ω_i^2 in the ith position. Consequently,

$$K^{-1} = \phi\Omega^{-1}\phi^T = \phi^m(I + E^T)(\Omega^{m^{-1}} + \Omega_E^{-1})(I + E)\phi^{mT} \tag{14}$$

where Ω_E^{-1}, the error in Ω^{-1}, is a diagonal matrix with $-2e_i/\omega_i^{m3}$ in the ith position (neglecting second-order terms in e_i). Neglecting second-order effects, Eq. (14) may be written as

$$(K^{-1})_E = \phi^m(E^T\Omega^{m^{-1}} + \Omega^{m^{-1}}E)\phi^{mT} + \phi^m\Omega_E^{-1}\phi^{mT} \tag{15}$$

By using the equivalent of Eq. (11) for the stiffness matrix, we finally obtain

$$K_E = -K_m\phi^m(E^T\Omega^{m^{-1}} + \Omega^{m^{-1}}E)\phi^{mT}K^m - K^m\phi^m\Omega_E^{-1}\phi^{mT}K^m \tag{16}$$

To conclude this section, we note that the diagonal terms e_{ii} in the modal error matrix indicate errors in the magnitude of a mode rather than its shape. This error effectively translates to an error in the modal mass which is usually quite small, so it was assumed that $e_{ii} = 0$. Mathematically, this is equivalent to the assumption that

$$\phi_i^T M^m \phi_i = 1 \tag{17}$$

Low Damping Analysis

Even with active controls many large space structures are expected to be only lightly damped. For such lightly damped structures, it is possible to estimate the complex eigenvalues by treating the damping matrix as a perturbation. That is, we can use Eq. (6) with C replacing C_E and the nominal eigenvalue and eigenvector being $i\omega_r$ and ϕ_r to yield

$$\lambda_r = i\omega_r - \frac{i\omega_r\phi_r^T C\phi_r}{2i\omega_r\phi_r^T M\phi_r} = i\omega_r - \frac{\phi_r^T C\phi_r}{2} \tag{18}$$

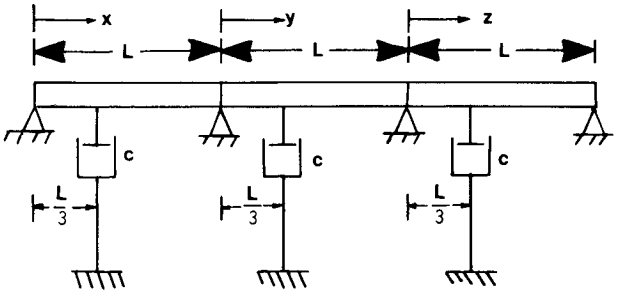

Fig. 1 A three-segment beam with dampers ($L = 50$ in., $A = 0.125$ in.^{2}, $E = 1.0 \times 10^6$ lb/in.^{2}, $I = 4.0 \times 10^{-5}$ in.^{4}, $\gamma = 0.28$ lb/in.^{3}).

If we now use Eq. (2), we find that the first-order effect of errors in the mode shapes is

$$\lambda_{rE} = ie_r - \sum_j e_{rj}\phi_r^{m\,T} C \phi_j^m \tag{19}$$

Equation (19) shows that errors in frequency do not have any first-order effect on the error in the real part of λ_r.

This analysis of the behavior of lightly damped structures is satisfactory except in the case of closely spaced modes. There, even though the effect of frequency errors on the real part of λ_r is a second-order effect, it can have a significant impact. When only two modes are closely spaced, the effect of frequency errors on the real part of the eigenvalue can be estimated by performing a two-mode analysis (reducing the system to a two-degree-of-freedom problem), neglecting the contribution of all other modes.

Results and Discussion

A Three-Span Simply Supported Beam

The first example considered was a three-span simply supported beam with three pairs of direct-rate feedback colocated sensors and actuators represented as viscous dampers as shown in Fig. 1. As a first step, the natural frequencies of the system were obtained exactly. To that end, the general expression for the transverse deflection w was written for each of the three spans.

$$w_1(x) = C_1\sin\lambda x + C_2\cos\lambda x + C_3\sinh\lambda x + C_4\cosh\lambda x \tag{20a}$$

$$w_2(y) = C_5\sin\lambda y + C_6\cos\lambda y + C_7\sinh\lambda y + C_8\cosh\lambda y \tag{20b}$$

$$w_3(z) = C_9\sin\lambda z + C_{10}\cos\lambda z + C_{11}\sinh\lambda z + C_{12}\cosh\lambda z \tag{20c}$$

Table 1 Natural frequencies of undamped three-span beam (radian/s)

	Perfect beam		Imperfect beam	
	Finite element	Analytic	Analytic $n=1$	(Rayleigh-Ritz) $n=2$
1	2.6242	2.6221	2.7076	2.6157
2	3.3647	3.3496	3.4732	3.3594
3	4.9204	4.8717	5.0985	4.9179
4	10.614	10.488	10.822	10.435
5	12.129	11.916	12.289	11.984
6	14.955	14.563	15.234	14.704
7	26.192	23.599	24.342	23.415
8	28.874	25.692	26.470	25.883
9	34.433	29.492	30.853	29.792
10	48.703	41.954	43.267	41.534
11	55.096	44.702	46.035	45.091
12	66.653	49.634	51.926	50.169
13	87.144	65.552	67.594	64.774
14	99.480	68.943	70.798	69.611
15	113.842	75.003	78.455	75.851

where the coordinates x, y, and z are shown in Fig. 1, and the parameter λ is given as

$$\lambda^4 = \left(\frac{m\omega^2}{EI}\right) \tag{21}$$

where m is the mass per unit length of the beam, EI is its bending rigidity, and ω is the natural frequency. Note that each of the three spans were assumed to have the same mass per unit length and the same bending rigidity.

The natural frequencies and the mode shapes of the three-span beam were obtained by satisfying the appropriate boundary conditions at the two extreme ends and appropriate compatibility and equilibrium equations at the two inner supports. These conditions can be expressed as

$$w_1(0) = 0 \tag{22a}$$

$$w_1''(0) = 0 \tag{22b}$$

$$w_1(L) = 0 \tag{22c}$$

$$w_2(0) = 0 \tag{22d}$$

$$w_1'(L) = w_2'(0) \tag{22e}$$

$$w_1''(L) = w_2''(0) \tag{22f}$$

$$w_2(L) = 0 \tag{22g}$$

$$w_3(0) = 0 \tag{22h}$$

$$w_2'(L) = w_3'(0) \tag{22i}$$

$$w_2''(L) = w_3''(0) \tag{22j}$$

$$w_3(L) = 0 \tag{22k}$$

$$w_3''(L) = 0 \tag{22l}$$

Satisfying the above equations leads to a set of 12 equations in the coefficients C_i and λ. These equations in matrix form can be written as

$$[K(\lambda L)]\{C\} = \{0\} \tag{23}$$

The set of equations will have a solution, if the determinant of the matrix $K(\lambda L)$ is equated to zero.

$$|K(\lambda L)| = 0 \tag{24}$$

Equation (24) gives the characteristic equation. The natural frequencies are obtained by solving the above equation for values of λL which in turn yield the natural frequencies. Table 1 gives the natural frequencies of the beam for the first 15 modes. The results obtained using nine finite elements are also

Table 2 Eigenvalues for the controlled system (perfect case)

	$c = 0.005$			$c = 0.0017$	
Mode number	Analytical results (complex eigenvalue analysis)	Eq. (18) (real part)	Finite-element results	Analytical results (complex eigenvalue analysis)	Eq. (18) (real part)
1	$-0.852 \pm j\ 2.521$	-0.827	$-0.855 \pm j\ 2.523$	$-0.282 \pm j\ 2.611$	-0.281
2	$-0.843 \pm j\ 3.303$	-0.828	$-0.848 \pm j\ 3.289$	$-0.282 \pm j\ 3.370$	-0.282
3	$-0.856 \pm j\ 4.9636$	-0.834	$-0.866 \pm j\ 4.914$	$-0.284 \pm j\ 4.969$	-0.284
4	$-0.810 \pm j\ 10.328$	-0.827	$-0.850 \pm j\ 10.44$	$-0.281 \pm j\ 10.47$	-0.281
5	$-0.847 \pm j\ 11.864$	-0.859	$-0.898 \pm j\ 11.96$	$-0.292 \pm j\ 12.00$	-0.292
6	$-0.966 \pm j\ 14.73$	-0.970	$-1.044 \pm j\ 14.81$	$-0.330 \pm j\ 14.838$	-0.330
7	$0 \pm j\ 23.60$	0	$0 \pm j\ 26.21$	$0 \pm j\ 23.598$	0
8	$-0.166 \pm j\ 25.898$	-0.170	$-0.165 \pm j\ 28.86$	$-0.0578 \pm j\ 25.920$	-0.0578
9	$-0.203 \pm j\ 30.072$	-0.204	$-0.246 \pm j\ 34.43$	$-0.0693 \pm j\ 30.086$	-0.0693

shown in Table 1. As expected, the two sets of results are in good agreement with each other for first few (6) modes.

Eigenvalues of Controlled System

The natural frequencies and the mode shapes obtained for the undamped case were then used to obtain the eigenvalues of the controlled system. Two different values of the damping coefficients for each of the three dampers were used; namely, $c = 0.005$ and $c = 0.0017$ lb-s/in. The eigenvalues of the controlled system were obtained using two different methods: 1) an eigenvalue analysis and 2) using Eq. (18) which assumes the damping matrix to be a perturbation to the original system. Table 2 gives the eigenvalues of the damped system as obtained using the two methods. As expected, the two methods yield almost identical results (real parts of the eigenvalues) for the case of low damping. For the case of higher damping, the two sets of results are slightly different (2–3%) from each other. For the case of higher damping, eigenvalues were also obtained using nine finite elements. For the first six modes, all sets of results were found to be in good agreement.

Eigenvalues of the Imperfect System

The effect of small imperfections in the geometric properties of the beam on the eigenvalues of the controlled system was next studied. The objective of this study was to show that for known errors in the model the approximate analysis in terms of modal errors predicts well the errors in the damped eigenvalues. The imperfect beam was considered to have sinusoidal imperfections in both the width $b(x)$ and the height $t(x)$. These imperfections were taken as

$$b(x) = b_0\left(1 + \epsilon_b \sin\frac{n\pi x}{3L}\right) \tag{25a}$$

$$t(x) = t_0\left(1 + \epsilon_t \sin\frac{n\pi x}{3L}\right) \tag{25b}$$

The values for both ϵ_b and ϵ_t were taken to be 0.05. Two different values of n were considered; namely $n = 1$, and $n = 2$.

As a first step, natural frequencies of the undamped imperfect beam were obtained using the Rayleigh-Ritz method. The mode shapes of the undamped perfect case were considered as the displacement functions, i.e.,

$$\phi^{im}(x) = \sum_{j=1}^{N} \eta_j \phi_j(x) \tag{26}$$

where $\phi^{im}(x)$ is the mode shape for the imperfect beam, $\phi_j(x)$ is the jth mode for perfect beam and is normalized with respect

Table 3 Mode shapes of the imperfect structure (n = 1)

Mode number of perfect case	Mode number of the imperfect beam					
	1	2	3	4	5	6
1	0.9685	—	0.7055×10^{-2}	—	0.3556×10^{-2}	—
2	—	0.9771	—	0.4659×10^{-2}	—	-0.1464×10^{-2}
3	0.1675×10^{-1}	—	0.9631	—	0.7169×10^{-3}	—
4	—	0.1067×10^{-1}	—	0.9691	—	-0.1312×10^{-1}
5	0.4012×10^{-2}	—	0.1391×10^{-1}	—	0.9753	—
6	—	0.2878×10^{-2}	—	0.3489×10^{-1}	—	0.9628
7	0.3154×10^{-3}	—	—	—	0.1808×10^{-1}	—
8	—	—	—	0.8054×10^{-2}	—	0.2122×10^{-1}
9	—	—	0.2508×10^{-3}	—	0.5454×10^{-2}	—
10	—	0.1891×10^{-3}	—	0.8111×10^{-3}	—	—
11	0.1088×10^{-3}	—	0.3828×10^{-3}	—	-0.2825×10^{-3}	—
12	—	0.1899×10^{-3}	—	—	—	0.4319×10^{-3}
13	—	—	—	—	0.4858×10^{-3}	—
14	—	—	—	0.3446×10^{-3}	—	0.7997×10^{-3}
15	—	—	-0.1058×10^{-3}	—	0.5026×10^{-3}	—
16	—	—	—	—	—	—
17	—	—	0.1092×10^{-3}	—	—	—
18	—	—	—	—	—	-0.2178×10^{-3}
19	—	—	—	—	—	—
20	—	—	—	—	—	0.2561×10^{-3}

— Indicates that the value is of the order of 10^{-5} or smaller.

Table 4 Mode shapes of the imperfect structure (n = 2)

Mode number of perfect case	Mode number of the imperfect beam					
	1	2	3	4	5	6
1	1.0004	0.5299×10^{-1}	—	0.1272×10^{-1}	0.1201×10^{-2}	0.3268×10^{-2}
2	-0.1192	0.9940	0.4808×10^{-1}	-0.2867×10^{-2}	0.1136×10^{-1}	—
3	0.6345×10^{-2}	-0.8659×10^{-1}	0.9972	0.6881×10^{-2}	—	0.4013×10^{-2}
4	0.1102×10^{-1}	0.2274×10^{-2}	-0.2732×10^{-1}	0.9833	0.1582	0.4543×10^{-2}
5	-0.1281×10^{-2}	0.8946×10^{-2}	0.2138×10^{-2}	-0.2153	0.9754	0.8131×10^{-1}
6	—	-0.1362×10^{-2}	0.2066×10^{-1}	0.1670×10^{-1}	-0.1224	0.9934
7	—	0.2049×10^{-2}	—	0.2087×10^{-1}	0.6606×10^{-2}	-0.3725×10^{-1}
8	0.1005×10^{-2}	—	0.2066×10^{-2}	-0.4194×10^{-2}	0.1648×10^{-1}	-0.4409×10^{-2}
9	—	—	—	—	-0.3133×10^{-2}	0.3132×10^{-1}
10	—	—	—	—	0.4281×10^{-2}	-0.1179×10^{-2}
11	—	—	—	0.2554×10^{-2}	—	0.3688×10^{-2}
12	—	—	—	—	0.1504×10^{-2}	—
13	—	—	—	—	—	—
14	—	—	—	—	—	—
15	—	—	—	—	—	—
16	—	—	—	—	—	—
17	—	—	—	—	—	—

— Indicates that the value is of the order of 10^{-4} or less.

to the mass matrix of the perfect beam, and η_j is the jth generalized coordinate. The natural frequencies for the first 15 modes for the two imperfect beams, obtained using $N = 30$, are shown in Table 1. The values of the coefficients η_j for the first six modes of the imperfect three-span beams are shown in Tables 3 and 4. The coefficients η_j were obtained by normalizing these with respect to the mass matrix of the imperfect beam $[M]$ i.e., for the ith mode:

$$\{\eta\}^T[M]\{\eta\} = 1 \tag{27}$$

The matrix $[M]$ is given as

$$M_{ij} = \int \zeta t(x)b(x)\phi_i(x)\phi_j(x)\,dx \tag{28}$$

It is clear that the mode shape for a given mode is dominated by the mode shape of the corresponding mode of the perfect beam.

The eigenvalues of the controlled imperfect system were next obtained. These are given in Table 5 for $c = 0.0005$ and in Table 6 for $c = 0.0015$. For the sake of comparison, the eigenvalues for the perfect case are also given in these tables. It is clear that the real part of the eigenvalue (a measure of the controlled response) is sensitive to the modeling errors.

The real parts of the eigenvalues also proved to be sensitive to the number of modes used in the Rayleigh-Ritz analysis. Because of the numerical problems associated with the hyperbolic functions, only 30 modes of the perfect structure could be obtained. This number may not be sufficient for convergence of the real part of the higher modes in Tables 5 and 6.

The real part of an eigenvalue can also be obtained using Eq. (19). This equation predicts the error in the real part of the given eigenvalue of the controlled system due to errors in the mode shapes. In the present example, the differences between the mode shapes of the perfect and imperfect structures can be considered as errors in modeling. Based on these differences (in the mode shapes) and using Eq. (19), the differences between the real parts of the eigenvalues of the two systems were obtained which in turn yielded the real parts of the eigenvalues of the imperfect (or true) structure. These results are also shown in Tables 5 and 6.

For the case of $n = 1$ [see Eqs. (25)], it is noted that, for both the damping levels, almost identical results are obtained using Eq. (19) and from an eigenvalue reanalysis. For the case of $n = 2$, however, significant differences can be observed to be

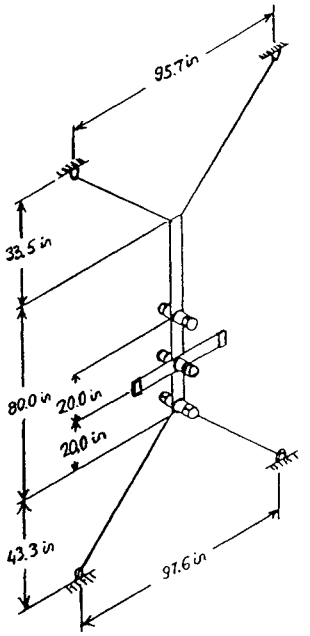

Fig. 2 Drawing of the laboratory structure.

Table 5 Eigenvalues for the controlled system, perfect and imperfect cases ($c = 0.0005$)

Mode number	Perfect case: Complex eigenvalue analysis (CEA)	Imperfect case ($n = 1$): Eq. (19), real part	Imperfect case ($n = 1$): CEA	Imperfect case ($n = 2$): Eq. (19), real part	Imperfect case ($n = 2$): CEA
1	$-0.0827 \pm j\ 2.621$	-0.0775	$-0.0776 \pm j\ 2.707$	-0.0807	$-0.0819 \pm j\ 2.615$
2	$-0.0828 \pm j\ 3.362$	-0.0790	$-0.0791 \pm j\ 3.473$	-0.0821	$-0.0830 \pm j\ 3.359$
3	$-0.0834 \pm j\ 4.913$	-0.0772	$-0.0773 \pm j\ 5.098$	-0.0788	$-0.0790 \pm j\ 4.918$
4	$-0.0827 \pm j\,10.49$	-0.0775	$-0.0776 \pm j\,10.82$	-0.0901	$-0.0943 \pm j\,10.43$
5	$-0.0859 \pm j\,11.96$	-0.0812	$-0.0813 \pm j\,12.29$	-0.0802	$-0.0838 \pm j\,11.98$
6	$-0.0966 \pm j\,14.68$	-0.0878	$-0.0879 \pm j\,15.23$	-0.0943	$-0.0947 \pm j\,14.70$
7	$0 \pm j\,23.60$	0	$-0.00009 \pm j\,24.34$	0	$-0.00172 \pm j\,23.42$
8	$-0.0151 \pm j\,25.78$	-0.0152	$-0.0151 \pm j\,26.47$	-0.0131	$-0.0135 \pm j\,25.88$
9	$-0.0180 \pm j\,29.73$	-0.0181	$-0.0179 \pm j\,30.85$	-0.0208	$-0.0213 \pm j\,29.79$
10	$-0.0827 \pm j\,41.95$	-0.0773	$-0.0776 \pm j\,43.27$	-0.0619	$-0.0726 \pm j\,41.53$
11	$-0.0703 \pm j\,44.86$	-0.0660	$-0.0663 \pm j\,46.03$	-0.0675	$-0.0774 \pm j\,45.09$
12	$-0.0602 \pm j\,50.28$	-0.0559	$-0.0564 \pm j\,51.93$	-0.0525	$-0.0558 \pm j\,50.17$

Table 6 Eigenvalues for the controlled system, perfect and imperfect cases ($c = 0.0015$)

Mode number	Perfect case: Complex eigenvalue analysis (CEA)	Imperfect case ($n = 1$): Eq. (19), real part	Imperfect case ($n = 1$): CEA	Imperfect case ($n = 2$): Eq. (19), real part	Imperfect case ($n = 2$): CEA
1	$-0.249 \pm j\ 2.614$	-0.233	$-0.233 \pm j\ 2.700$	-0.243	$-0.246 \pm j\ 2.607$
2	$-0.249 \pm j\ 3.356$	-0.238	$-0.238 \pm j\ 3.468$	-0.247	$-0.249 \pm j\ 3.354$
3	$-0.251 \pm j\ 4.913$	-0.232	$-0.232 \pm j\ 5.098$	-0.237	$-0.237 \pm j\ 4.918$
4	$-0.247 \pm j\,10.47$	-0.231	$-0.233 \pm j\,10.81$	-0.269	$-0.283 \pm j\,10.42$
5	$-0.257 \pm j\,11.95$	-0.243	$-0.244 \pm j\,12.28$	-0.240	$-0.251 \pm j\,11.97$
6	$-0.290 \pm j\,14.67$	-0.264	$-0.264 \pm j\,15.22$	-0.283	$-0.284 \pm j\,14.69$
7	$0 \pm j\,23.60$	0	$-0.0003 \pm j\,24.34$	0	$-0.0051 \pm j\,23.41$
8	$-0.0454 \pm j\,25.78$	-0.0456	$-0.0452 \pm j\,26.47$	-0.0393	$-0.0403 \pm j\,25.88$
9	$-0.0539 \pm j\,29.73$	-0.0542	$-0.0535 \pm j\,30.85$	-0.0624	$-0.0640 \pm j\,29.79$
10	$-0.248 \pm j\,41.95$	-0.232	$-0.233 \pm j\,43.26$	-0.185	$-0.218 \pm j\,41.53$
11	$-0.210 \pm j\,44.86$	-0.197	$-0.199 \pm j\,46.03$	-0.202	$-0.232 \pm j\,45.09$
12	$-0.181 \pm j\,50.03$	-0.168	$-0.169 \pm j\,51.92$	-0.158	$-0.167 \pm j\,50.17$

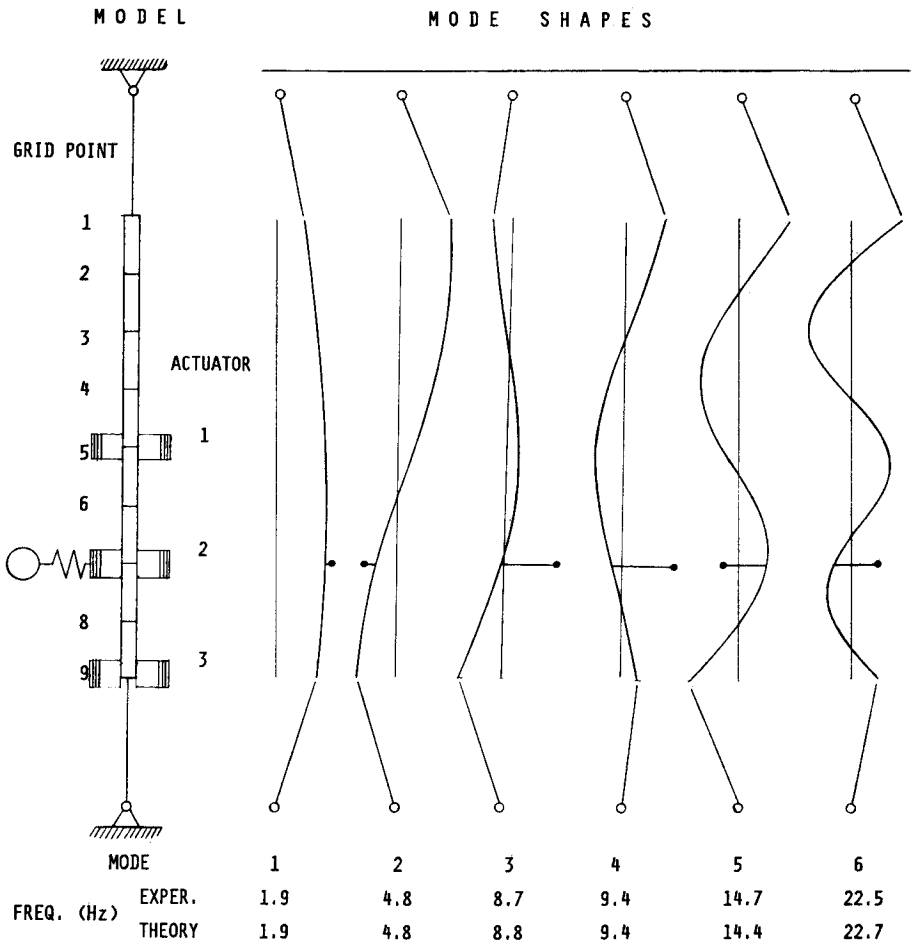

Fig. 3 Finite-element model and mode shapes.

Table 7 Analytical and experimental frequencies and damping ratios for cruciform beam structure

Mode number	Natural frequencies, Hz		Damping ratio, ζ		
	Experimental	Analytical	Experimental	Full analysis	Eq. (18)
1	1.9	1.9	0.219	0.214	0.213
2	4.8	4.8	0.040	0.045	0.045
3	8.7	8.8	0.050	0.075	0.066
4	9.4	9.5	0.036	0.030	0.038
5	14.7	14.4	0.024	0.029	0.029
6	22.5	22.7	0.029	0.030	0.029

for higher modes, especially for modes that have close natural frequencies (e.g., modes 4 and 5 with $\omega_5/\omega_4 = 1.148$; and modes 10 and 11 with $\omega_{11}/\omega_{10} = 1.085$). An apparent exception appears to be the results of damped characteristics for closely spaced modes 8 and 9 with frequency ratio $\omega_9/\omega_8 = 1.151$. For these modes, the results given by Eq. (19) are in good agreement with those obtained from a complete reanalysis. This can be attributed to the fact that the damping levels (i.e., the real part of the complex eigenvalues) for these modes are much smaller than those for other closely spaced modes, namely, 4 and 5 and 10 and 11. Since damping is the mechanism coupling the modes, lighter damping means less coupling and a smaller effect of the closeness of the two frequencies.

These differences for closely spaced modes are probably due to the slow convergence of the real part of the eigenvalues observed also in Ref. 5 for closely spaced modes.

Cruciform Beam Suspended by Cables

As a second example, the proposed procedure was applied to a laboratory structure consisting of a cruciform beam suspended by cables (Fig. 2). The beam is controlled by three rate-feedback colocated force-actuator velocity-sensor pairs. The control system was designed in Ref. 2 to produce uncoupled controllers which act as electromagnetic dashpots. The beam was analyzed by a finite-element model shown in Fig. 3, and the damping matrix corresponding to the three actuators consisted of a diagonal matrix with three nonzero entries corresponding to the three sensed velocities.

Table 7 compares the experimental and analytical results from Ref. 2 with the approximate damping ratio obtained from Eq. (18). It is seen that except for modes 3 and 4 the approximate results are identical with the exact finite-element results. Modes 3 and 4 are closely coupled with $\omega_4/\omega_3 = 1.08$, and this explains why the approximate analysis does not predict their damping ratios correctly. It is interesting to note, however, that the uncoupled approximation to the damping ratio, obtained from Eq. (18), is closer to the experimental results than the full-analysis results. This may indicate that the coupling between the two modes is exaggerated by the analytical model. A two-mode approximation gives a damping ratio of 0.073 for the third mode and 0.031 for the fourth.

Next, the sensitivities of the damping ratios to errors in mode shapes and frequencies are presented in Table 8. The table presents the sensitivity of each damping ratio to errors in

Table 8 Sensitivity of damping ratios ζ_i to errors in mode shapes e_{ij} and frequencies e_i for cruciform beam structure (percent change in ζ due to 1% error in mode shape or frequency)

Mode number i	Maximum sensitivity $\frac{\partial \zeta_i}{\partial e_{ij}}(j)$ Eq. (19)	Maximum sensitivity $\frac{\partial \zeta_i}{\partial e_{ij}}(j)$ Full analysis	$\frac{\partial \zeta_i}{\partial e_j}(j)$
1	2.2	1.8 (6)	−0.54 (1)
2	3.1	3.0 (3)	−0.93 (2)
3	1.5	1.8 (8)	2.1 (4)
4	2.5	2.5 (6)	5.1 (3)
5	2.0	1.9 (6)	−0.99 (5)
6	1.3	1.3 (1)	−0.85 (6)

Table 9 Effect of ratio of fourth and third natural frequencies on damping ratios for cruciform beam

	ω_4/ω_3	ζ_3	ζ_4
	1.15	0.0689	0.0330
	1.125	0.0696	0.0331
	1.10	0.0711	0.0325
	1.09	0.0720	0.0318
(actual)	1.08	0.0734	0.0308
	1.07	0.0752	0.0293
	1.06	0.0776	0.0273
	1.05	0.0802	0.0251
	1.04	0.0828	0.0229
	1.03	0.0850	0.0211
	1.02	0.0867	0.0197

mode shapes and frequencies that it is most sensitive to. For example, the first damping ratio is primarily affected by errors in the first mode. The first line in the table indicates that an error in the first mode which is in shape of the sixth mode has the largest effect on the first damping ratio. Furthermore, a 1% contamination of the first mode by the sixth mode is predicted to change ζ_1 by 1.8% using the full analysis and by 2.2% using the approximation of Eq. (19).

The information contained in Table 8 is compatible with the observed differences between analytical and experimental damping ratios in Table 7. The typical measured error in mode shape was 5%, and this would translate to maximum errors in ζ of the order of 6–18%. The difference between analytical and experimental results is outside this range only for the third mode. However, because this mode is closely coupled to the fourth mode, the errors in the mode shape are expected to be substantially larger than 5%.

Without second-order effects (in the damping), all of the $\partial\zeta/\partial e_i$ would be equal to -1. That is, a 1% increase in natural frequency changes the complex frequency by the same amount without affecting the real part by much, so that the damping ratio is reduced by 1%. The actual numbers are substantially different only for the closely coupled third and fourth mode. For the fourth mode, a 1% increase in the third natural frequency would increase the damping ratio by 5.1%. This is a substantial amount that can account for about a quarter of the experimental-analytical discrepancy.

The cruciform beam was designed to have two close frequencies, but at 8% difference they are still far apart compared to what can be expected for large space structures. To see the effect of close frequencies on the damping ratios, the ratio of the two natural frequencies was varied without changing the mode shapes. The dependence of the damping ratios on the frequency ratio is given in Table 9. It is seen that the damping ratio of ζ_4 changes very rapidly when the ratio ω_4/ω_3 is about 1.05. This table emphasizes the importance of minimizing the damping coupling between modes of close frequency, so as to prevent extreme sensitivity of the damping ratio to frequency errors.

Concluding Remarks

In this paper, the sensitivity of the response of an actively damped structure to modeling errors is considered. The errors were considered using two different approaches. In the first approach, the errors were assumed in the form of spatial variations (or imperfections) in the mass and stiffness properties of the structure assumed during the design of the controller. The second approach was concerned with errors due to such factors as unknown joint stiffnesses, discretization errors, and nonlinearities. These types of errors were represented as discrepancies between experimental and analytical mode shapes and frequencies. The controlled system considered here was a simple direct-rate feedback regulator based on a number of velocity sensors and force actuators. The response of the controlled structure was characterized by the eigenvalues of the closed-loop system. The effect of modeling errors was studied as the sensitivity of the closed-loop eigenvalues to the changes in the eigenvalues and the mode shapes. The results were presented for two different examples: 1) a three-span simply supported beam with three actuators and sensors; and 2) a laboratory structure that consists of a cruciform beam controlled by a rate feedback, three-colocated force-actuator velocity-sensor pairs. For the first example, a good agreement is observed between the results obtained using the first approach—an approach in which the errors in the stiffness and inertial characteristics are explicitly known, and those obtained using the second approach—an approach in which the errors in the stiffness and inertial characteristics are only known in terms of the errors in the natural frequencies and mode shapes. The second example showed that the second approach can be used to understand better the experimental-analytical discrepancies in damping ratios.

Acknowledgment

This research was supported in part by NASA Grant NAG-1-224.

References

[1]NASA Scientific and Technical Information Branch, "Technology for Large Space Systems—A Bibliography with Index," NASA SP-7046(09), July 1983.

[2]Haftka, R. T., Martinovic, Z. N., and Hallauer, W. L., Jr., "Enhanced Vibration Controllability by Minor Structural Modifications," *AIAA Journal,* Vol. 23, Aug. 1985, pp. 1260–1266.

[3]Haftka, R. T., Martinovic, Z. N., Hallauer, W. L., Jr., and Schamel, G. S., "An Analytical and Experimental Study of the Sensitivity of Control Systems to Structural Modifications," *AIAA Journal,* Vol. 25, Jan. 1987, pp. 134–138.

[4]Wang, B. P. and Pilkey, W. D., "Eigenvalue Reanalysis of Locally Modified Structures Using a Generalized Rayleigh's Method," *AIAA Journal,* Vol. 24, June 1986, pp. 983–990.

[5]Sandridge, C. A. and Haftka, R. T., "Effect of Modal Truncation on Derivatives of Optimal Control Performance," International Conference on Computational Engineering Science, Atlanta, GA, Springer-Verlag, N.Y., April 1988.